

The Local Group Galaxy NGC 6822 and its Asymptotic Giant Branch Stars

Patricia A. Whitelock^{2,1}, John W. Menzies², Michael W. Feast^{1,2},
 Francois Nsengiyumva^{2,1}, and Noriyuki Matsunaga³

¹ *Astronomy, Cosmology and Gravity Centre, Astronomy Department, University of Cape Town, 7701 Rondebosch, South Africa.*

² *South African Astronomical Observatory, P.O.Box 9, 7935 Observatory, South Africa.*

³ *Kiso Observatory, Institute of Astronomy, The University of Tokyo, 10762-30, Mitake, Kiso, Nagano 397-0101, Japan.*

1 September 2018

ABSTRACT

JHK_S photometry is presented from a 3.5 year survey of the central regions of the irregular galaxy NGC 6822. The morphology of the colour-magnitude and colour-colour diagrams is discussed with particular reference to M, S and C-type AGB stars and to M-supergiants. Mean *JHK_S* magnitudes and periods are given for 11 O-rich and 50 presumed C-rich Miras. Data are also listed for 27 large amplitude AGB stars without periods and for 69 small amplitude AGB variables. The slope of the bolometric period-luminosity relation for the C-rich Miras is in good agreement with that in the LMC. Distance moduli derived from the C- and O-rich Miras are in agreement with other estimates. The period distribution of C-rich Miras in NGC 6822 is similar to that in the Magellanic Clouds, but differs from that in the dwarf spheroidals in the Local Group. In the latter there is a significant proportion of large amplitude, short period variables indicating a population producing old carbon-rich AGB stars.

Key words: stars: variables: AGB; stars: carbon; galaxies: distances and redshifts; galaxies: individual: NGC 6822; (galaxies:) Local Group; infrared: stars

1 INTRODUCTION

NGC 6822 is an isolated barred dwarf irregular galaxy within the Local Group. It is comparable in size to the SMC but has a slightly higher metallicity (Muschielok et al. 1999; Venn et al. 2001). It contains numerous supergiants and HII regions with obvious signs of star formation and is sometimes referred to as a polar ring galaxy (Demers et al. 2006). Recent HST colour-magnitude studies suggest that over 50 percent of its stars formed in the last 5 Gyr (Cannon et al. 2012).

We present here new multi-epoch *JHK_S* photometry of the central regions of NGC 6822 which we compare with earlier work and use to identify and characterize large amplitude, Mira, asymptotic giant branch (AGB) variables. Earlier papers used the same photometry to identify the first symbiotic star in NGC 6822 (Kniazhev et al. 2009) and to study the Cepheid variables (Feast et al. 2012). A preliminary analysis of the AGB variables was produced by Nsengiyumva (2010).

Earlier studies of red giants and AGB stars in NGC 6822 have been made by Cioni & Habing (2005), Kang (2006), Groenewegen et al. (2009), Kacharov, Rejkuba & Cioni (2012) and by Sibbons et al. (2012), while Battinelli & Demers (2011) specifically identified AGB variables.

This work forms part of a broad study of AGB variables in Local Group Galaxies which so far has covered Leo I (Menzies et al. 2002; 2010), Phoenix (Menzies et al. 2008), Fornax (Whitelock et al. 2009) and Sculptor (Menzies et al. 2011). These new observations provide an opportunity to compare these dwarf spheroidals with a dwarf irregular surveyed in the same way.

2 OBSERVATIONS

Our survey of NGC 6822 is confined to the optical bar which is aligned nearly N-S. We used the Japanese-South African IRSF telescope equipped with the SIRIUS camera, which permits simultaneous imaging in the *J*, *H* and *K_S* bands (see Nagayama et al. (2003) for details). We defined 3 overlapping fields, with field 1 centred at $\alpha(2000.0) = 19^{\text{h}}44^{\text{m}}56^{\text{s}}$ and $\delta(2000.0) = -14^{\circ}48'06''$. Fields 2 and 3 are centred 6.7 arcmin N and S, respectively, of field 1. The three fields, each approximately 7.8 arcmin square, were observed in *JHK_S* at 19, 18 and 16 epochs, respectively, over a period of 3.5 years.

Further details, including those of the photometric calibration, are given by Feast et al. (2012). The basic data for

arXiv:1210.3695v1 [astro-ph.GA] 13 Oct 2012

Table 1. Data for stars with standard errors less than 0.1 mag (note that this selection omits the large amplitude variables which are listed in various tables below). The full table is available on-line. The first two columns are the equatorial coordinates in degrees; N is our own identification number; the mean photometry, JHK_S is listed together with its standard deviation, δJHK_S ; NJ, NH and NK are the number of observations used to derive the means.

RA (2000.0)	Dec	N	J	δJ	H	δH	K_S (mag)	δK	$J - H$	$H - K_S$	$J - K_S$	NJ	NH	NK
296.28656	-14.80424	10001	12.613	0.009	12.050	0.006	11.939	0.026	0.563	0.111	0.674	18	14	18
296.17661	-14.78323	10002	12.704	0.014	12.303	0.016	12.217	0.030	0.401	0.086	0.487	18	18	18
296.18298	-14.83667	10008	13.354	0.018	12.903	0.008	12.819	0.033	0.451	0.084	0.535	18	16	18
296.20160	-14.83465	10009	13.602	0.009	13.112	0.004	13.020	0.021	0.490	0.092	0.582	18	12	18
296.21399	-14.82684	10010	13.161	0.009	12.751	0.009	12.673	0.012	0.410	0.078	0.488	17	17	18

stars with standard errors less than 0.1 mag in each band are provided on-line, and the first few lines of the catalogue are illustrated in Table 1 (The Mira variables, discussed in section 5, are not in this table). Numbers of observations, NJ, NH etc. larger than 19 are found for some stars in the areas of overlap between fields.

NGC 6822 is at low galactic latitude, $b = -18^\circ.4$, so it experiences some interstellar extinction as well as confusion with Galactic sources. For the interstellar extinction we adopt $A_V = 0.77$ mag (amounting to $A_J = 0.20$, $A_H = 0.12$, $A_K = 0.07$ mag) from Clementini et al. (2003) using the information from Schlegel, Finkbeiner & Davis (1998). We note, however, that the extinction across NGC 6822 is somewhat variable and that significantly higher values are possible for sources associated with star forming regions. Our discussion of the AGB, and of the large amplitude variables in particular, will not be very sensitive to either the reddening, or its variability.

3 COLOUR-MAGNITUDE DIAGRAM

The colour-magnitude and two-colour diagrams for stars from Table 1 plus the variables discussed in section 5, are illustrated in Fig. 1 and Fig. 2.

According to the detailed analysis by Sibbons et al. (2012) the tip of the red giant branch (TRGB) is at $K_0 = 17.42 \pm 0.11$ mag (2MASS system). So here we are dealing entirely with AGB stars, together with a sprinkling of red supergiants at the highest luminosity. Following Sibbons et al. we identify stars with $(J - H)_0 < 0.75$ mag as most likely to be foreground dwarfs and they are shown as gray, unless they have spectral types. Most, but not all, of the stars populating the left of the colour magnitude diagram and the bottom of the two-colour diagram are foreground dwarfs.

The morphology of these diagrams is more clearly understood when stars of known spectral type are identified and it is therefore discussed in the next section.

4 SPECTRAL TYPES

Various groups have attempted to separate the AGB stars into M- and C-type on the basis of their $J - K$ colour (Cioni & Habing (2005), Kang et al. (2006), Sibbons et al. (2012)). Kacharov et al. (2012) obtained spectra, including 148 stars

in common with us, two of which are Mira variables. They concluded that 79 percent of the carbon stars had $(J - K)_0 > 1.28$ mag (on the 2MASS system).

Letarte et al. (2002) obtained narrow band photometry over a very large field in order to find the extent of the NGC 6822 C-star population. Over 5000 stars were found in common with our sample including about 1000 with the colours of M stars ($R - I > 1.1$ and $CN - TiO < 0$) and 430 with the colours of C stars ($R - I > 1.1$ and $CN - TiO > 0.3$) and this allows a reasonably good division between M- and C-type stars among our variables (section 5). However, the central field is crowded and a few misidentifications are possible and might explain some outlying points among the C- and M- stars.

Levesque & Massey (2012) discuss red supergiants (RSGs) in NGC 6822 and use the $V - R$ and $B - V$ colours to separate RSGs from giants. Table 2 shows the photometry of the M-type supergiants from Levesque & Massey's table 2, which are also illustrated in Figs. 1 and 2. N10032 is a small amplitude variable (as the uncertainty on the mean magnitudes listed in Table 2 show). It is not obviously periodic and the full peak-to-peak amplitude is $\Delta K_S \sim 0.3$ mag. Note also that N10015 falls amongst the dwarfs in both figures, although its status as a supergiant is well established. As others have noted (Cioni & Habing 2005, see also Nikolaev & Weinberg 2000) there is no clear distinction in the colour-magnitude diagram between the giants and supergiants (or even between the supergiants and foreground dwarfs).

The broad morphology of Fig. 1 is now clear. The vertical strip between $(J - K)_0 \sim 0.3$ and 0.6 mag is mostly foreground stars, but will include warm supergiant members of NGC 6822, e.g., the Cepheids (section 5). The vertical strip around $(J - K_S)_0 \sim 0.9$ mag is mostly foreground M-dwarfs. The almost vertical strip at around $(J - K)_0 \sim 1.1$ mag starts just above the TRGB as M stars on the AGB; at higher luminosity, $K_{S0} < 15.8$ mag, it becomes luminous AGB stars. These stars are discussed further in the context of the variable stars (section 5), but are presumably younger than the bulk of the AGB population that evolve to the right of the diagram as C stars. It is here we would expect to find hot bottom burning stars (e.g. Sackman & Boothroyd 1992) and super-AGB stars (e.g. Siess 2008), prior to the onset of heavy mass-loss. At even higher luminosities, and between the AGB column and the M-dwarf column, fall the M supergiants. The carbon stars concentrate in a diagonal band to the right of the AGB M-type stars. The AGB variables

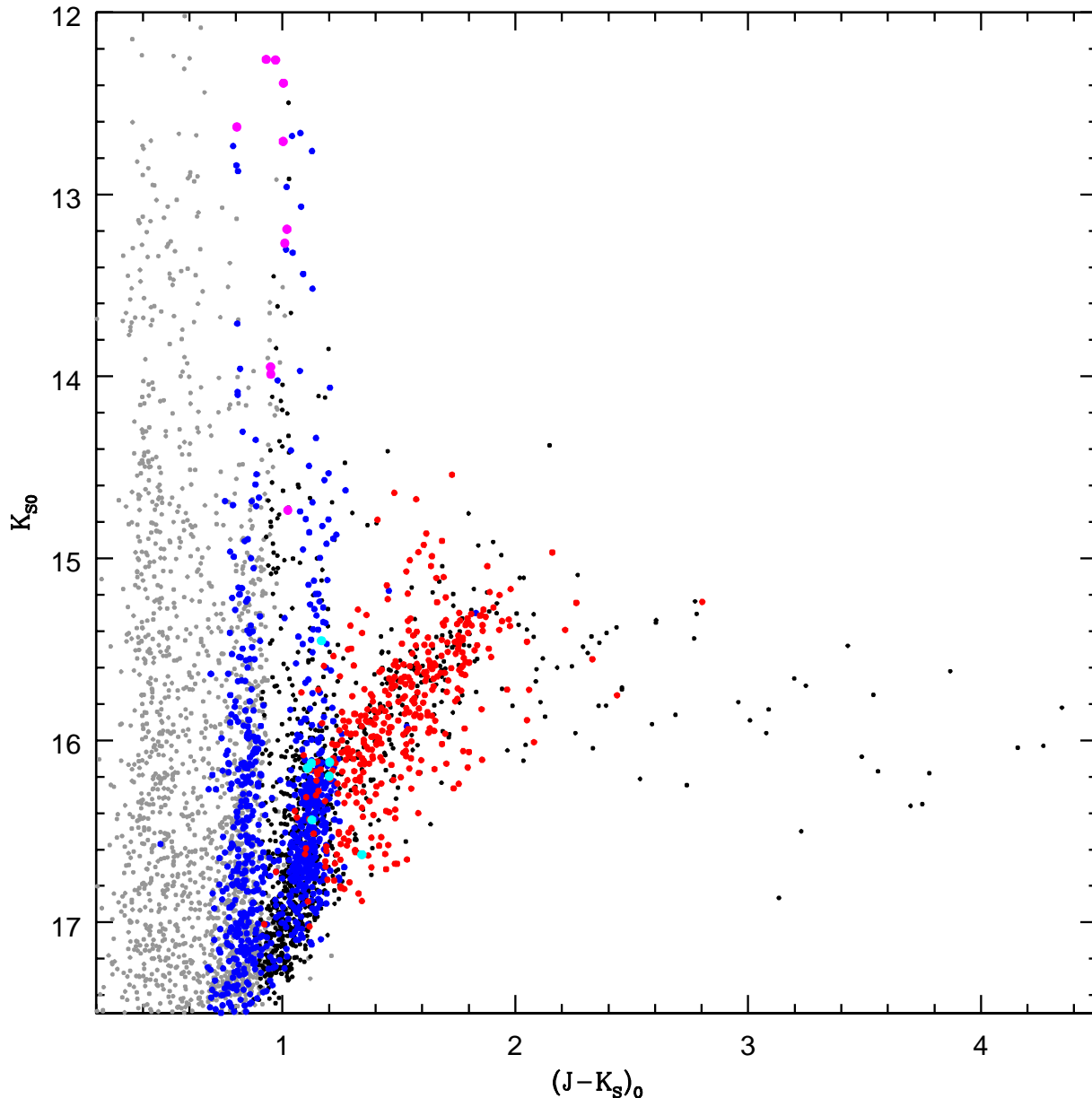


Figure 1. Colour-magnitude diagram showing the stars in our NGC 6822 catalogue in black and, for those that are probably foreground dwarfs, in gray (unless they have spectral types). The TRGB is at $K_0 = 17.42$ mag. Stars of known late spectral-type are shown in colour: those with narrow-band colours of M stars and C stars are shown in blue and red, respectively; S stars are shown in cyan and M supergiants in magenta.

without spectral types¹ extend the C-star sequence to the extreme right of the diagram. It is likely that a small number of the points below the carbon stars ($K_S > 16$ mag) in Fig. 1 are actually unresolved galaxies (see e.g. Whitelock et al. 2009).

¹ most of these will be C stars, but this is also the place we expect to find OH/IR stars if such objects exist in NGC 6822.

4.1 S stars

Six of the nine S stars identified by Kacharov et al. (2012) fall in the area we surveyed and they are listed in Table 3. All of these have the K_S magnitudes, and all but one have the colours, anticipated for an evolutionary state between that of the lower luminosity M stars and the C stars (see Fig. 1 and 2). The exception, N12050, has a slightly redder $J - K_S$ and therefore falls amongst the C stars (as noted by Kacharov et al.). The S star identified by Aaronson et al. (1984) is

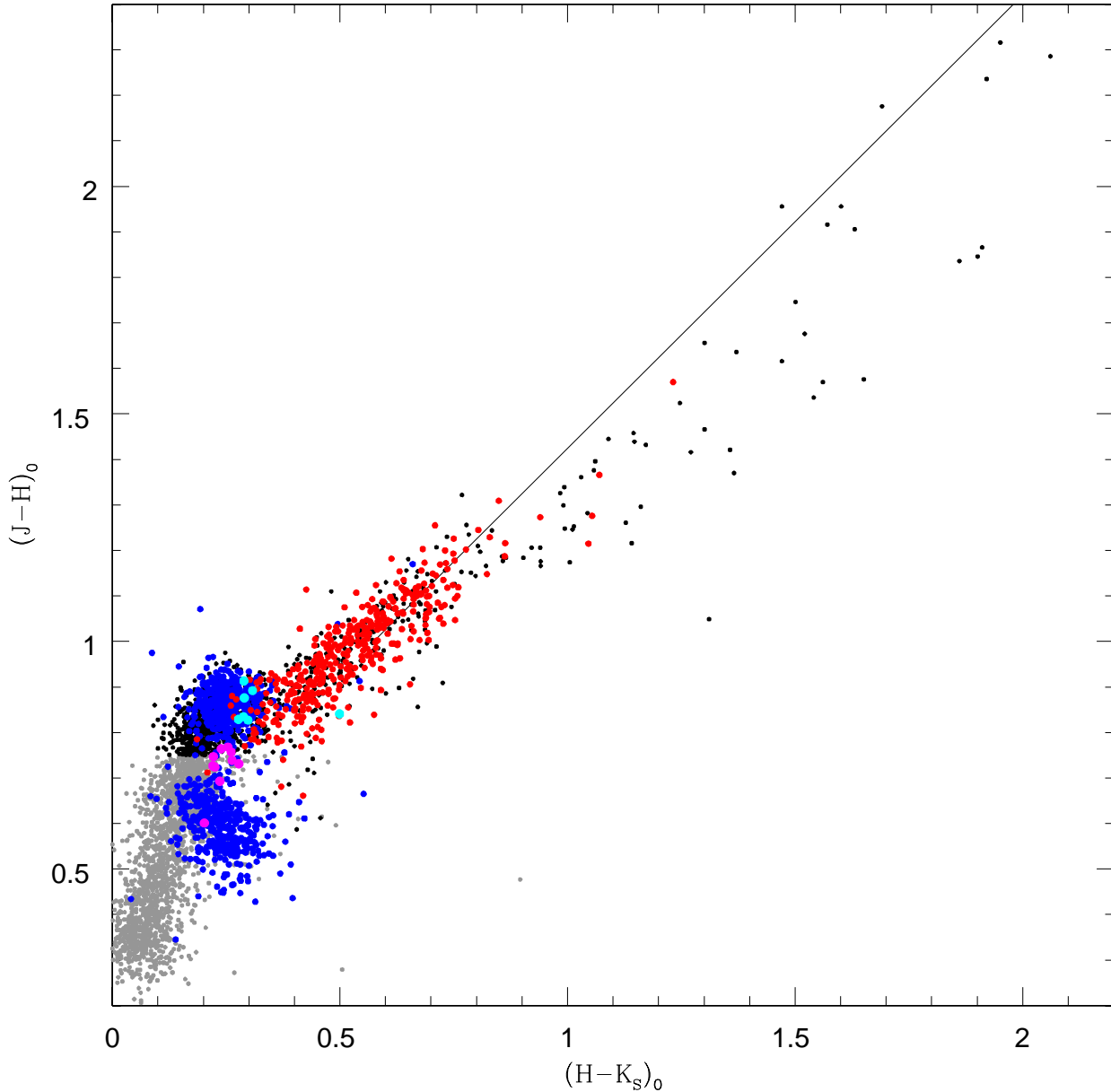


Figure 2. Two-colour diagram with the same stars as in Fig. 1. The line represents the locus for Galactic carbon Miras (equation 2 from Whitelock et al. (2006) converted to 2MASS as: $(H - K_S)_0 = 1.003(J - H)_0 - 0.428$). Note the very clear separation in $(J - H)_0$ of the foreground M-dwarfs (smaller values) and NGC 6822 M-giants (larger values). The M supergiants have intermediate colours.

our N10326 which is about a magnitude brighter than the Kacharov et al. S stars. If it is an intrinsic S star (i.e. its s-process elements are the consequence of its own evolution and dredge-up and are not from a close companion) then it must be more massive than the others, perhaps comparable to the hot bottom burning Li-rich S stars in the LMC and SMC (Smith et al. 1995; Whitelock et al. 2003). In that case it may be from the same population as the luminous large-amplitude O-rich variables discussed below.

5 VARIABLES

We examined the light curves of all stars with $K_S < 17$ mag for which we had at least 10 observations and which showed a standard deviation in J , H or K_S of > 0.2 mag, going to lower standard deviations for brighter magnitudes. By this approach we found the brightest of the Cepheids, all of the stars listed in Tables 4(a) and (b) plus a considerable fraction of those which we list in the later tables and which are discussed below. Given that our primary objective was to find large amplitude AGB variables we then examined

Table 2. M Supergiants from Levesque & Massey (2012).

LGGS	RA (2000.0)	Dec	N	J	δJ	H	δH (mag)	K_S	δK	$J - K_S$	NJ	NH	NK	Sp
J194445.76-145221.2	296.19067	-14.87276	30016	13.91	0.01	13.09	0.03	12.78	0.02	1.13	12	14	11	M1
J194447.81-145052.5	296.19919	-14.84817	40115	14.41	0.03	13.57	0.03	13.26	0.02	1.15	24	26	22	M1
J194450.44-144410.0	296.21021	-14.73628	40177	15.14	0.01	14.33	0.03	14.06	0.02	1.08	22	24	22	M2
J194453.46-144540.1	296.22278	-14.76476	10089	15.10	0.03	14.29	0.02	14.02	0.02	1.08	18	17	17	M4.5
J194454.46-144806.2	296.22696	-14.80191	10032	14.48	0.05	13.66	0.03	13.34	0.05	1.14	14	14	16	M1
J194454.54-145127.1	296.22726	-14.85778	40278	13.43	0.03	12.60	0.04	12.33	0.05	1.10	33	33	33	M0
J194455.70-145155.4	296.23212	-14.86564	40315	13.39	0.06	12.61	0.05	12.33	0.05	1.06	27	26	28	M0
J194457.31-144920.2	296.23883	-14.82247	10011	13.60	0.04	12.75	0.04	12.46	0.05	1.14	18	18	18	M1
J194459.86-144515.4	296.24945	-14.75443	10015	13.64	0.00	12.95	0.01	12.70	0.02	0.94	13	17	18	M1
J194503.58-144337.6	296.26492	-14.72723	20101	15.96	0.02	15.11	0.02	14.81	0.02	1.15	16	17	16	M0

Table 3. Stars with known S spectral-type.

RA (2000.0)	Dec	N	J	δJ	H	δH (mag)	K_S	δK	$J - K_S$	NJ	NH	NK
296.17892	-14.82286	10870	17.52	0.04	16.53	0.04	16.19	0.05	1.34	15	17	17
296.21545	-14.83469	10784	17.45	0.03	16.53	0.04	16.20	0.06	1.26	17	18	17
296.27341	-14.80861	11004	17.60	0.03	16.62	0.03	16.27	0.05	1.33	15	16	15
296.28308	-14.80497	11029	17.46	0.03	16.55	0.02	16.22	0.05	1.24	16	16	17
296.25427	-14.81764	12050	18.17	0.07	17.25	0.10	16.70	0.05	1.47	14	17	17
296.19156	-14.89296	30528	17.76	0.06	16.85	0.04	16.51	0.10	1.26	12	12	14
296.25522	-14.82579	10326	16.82	0.03	15.86	0.03	15.52	0.02	1.30	16	16	16

stars with $J - K_S > 2.2$ mag, finding them all to be variable at some level.

It should be noted that one consequence of the use of a reference frame in the H band to provide positions at which “fixed-position” DoPHOT photometry was performed (Feast et al. 2012) is that extremely red stars or stars with a very large amplitude of variation might have been missed. If the star was not measurable on the reference H frame, then it would not have been found in any other band either. This means that there may be red variables that we have not measured. The limiting magnitudes at J , H and K_S in our catalogue are approximately 20.3, 18.3 and 18.0 mag, respectively. This means that we would have missed red variables with $H - K_S = 2.0$ mag that were fainter than about $K_S = 16.3$ mag or $J = 18.4$ mag at the time the reference frame was obtained, even though these latter values are significantly above the relevant limiting magnitudes.

The various variables are identified in Figs. 3 and 4. The Cepheids were discussed by Feast et al. (2012) and the others are considered below.

Periods were determined by Fourier analysis and Table 4 lists the Fourier mean JHK_S magnitudes for the large amplitude (see below) variables with measurable periods (Miras), together with the peak-to-peak amplitudes. The table is split into (a) O-rich, M-type, stars and (b) C-stars, on the basis of $J - K_S$ colour (see section 4). Table 4 is the only one to list Fourier mean magnitudes. The other tables contain simple mean values of all the observations. Note that the stars in Table 4 are not in the online catalogue, because their mean magnitudes are evaluated differently.

Our previous practice has been to define large ampli-

tude, Mira, variables to be those with $\Delta K_S > 0.4$ mag (e.g. Whitelock et al. 2006). While the distinction between Miras and SR variables is clear for O-rich stars (Miras were originally defined from observations of Galactic stars, most of which are O-rich), it is not so clear for the C-rich stars (Whitelock 1996) and it is apparent that this cut-off results in far fewer short period ($P < 300$ days) Miras than we might expect in NGC 6822, and presumably in similar galaxies. However, if we are interested in these variables as distance indicators the distinction is important, because low-amplitude variables can fall on any one of several period-luminosity (PL) relations (Wood 2000, Ita et al. 2004) whereas the Miras with periods less than 450 days fall only on one relation. Nevertheless, we relax the criterion very slightly here to include stars with $0.36 < \Delta K_S < 0.4$ mag, while noting that we have done so in Table 4(b). The K_S light curves of the Mira variables are illustrated in the appendix.

With regard to establishing the O- or C-rich nature of the Miras, we follow Letarte et al. (2002) and relaxing their criteria (as they suggest) very slightly to examine stars with $R - I > 1.0$ (rather than 1.1) we find the following: 6 Miras have M-type narrow-band colours; they are labeled ‘M’ in the last column of Table 4(a), and all have $(J - K_S)_0 < 1.33$ mag. Similarly, 11 stars have C-type narrow-band colours; these are labeled ‘C’ in the last column of Table 4(b), and all have $(J - K_S)_0 > 1.33$ mag.

Two of the Miras have spectral types in Kacharov et al. (2012), as indicated in Table 4(b). N 12790 ($P=182$ days) has spectral type C6.5 and is the bluest ($(J - K_S)_0 = 1.31$

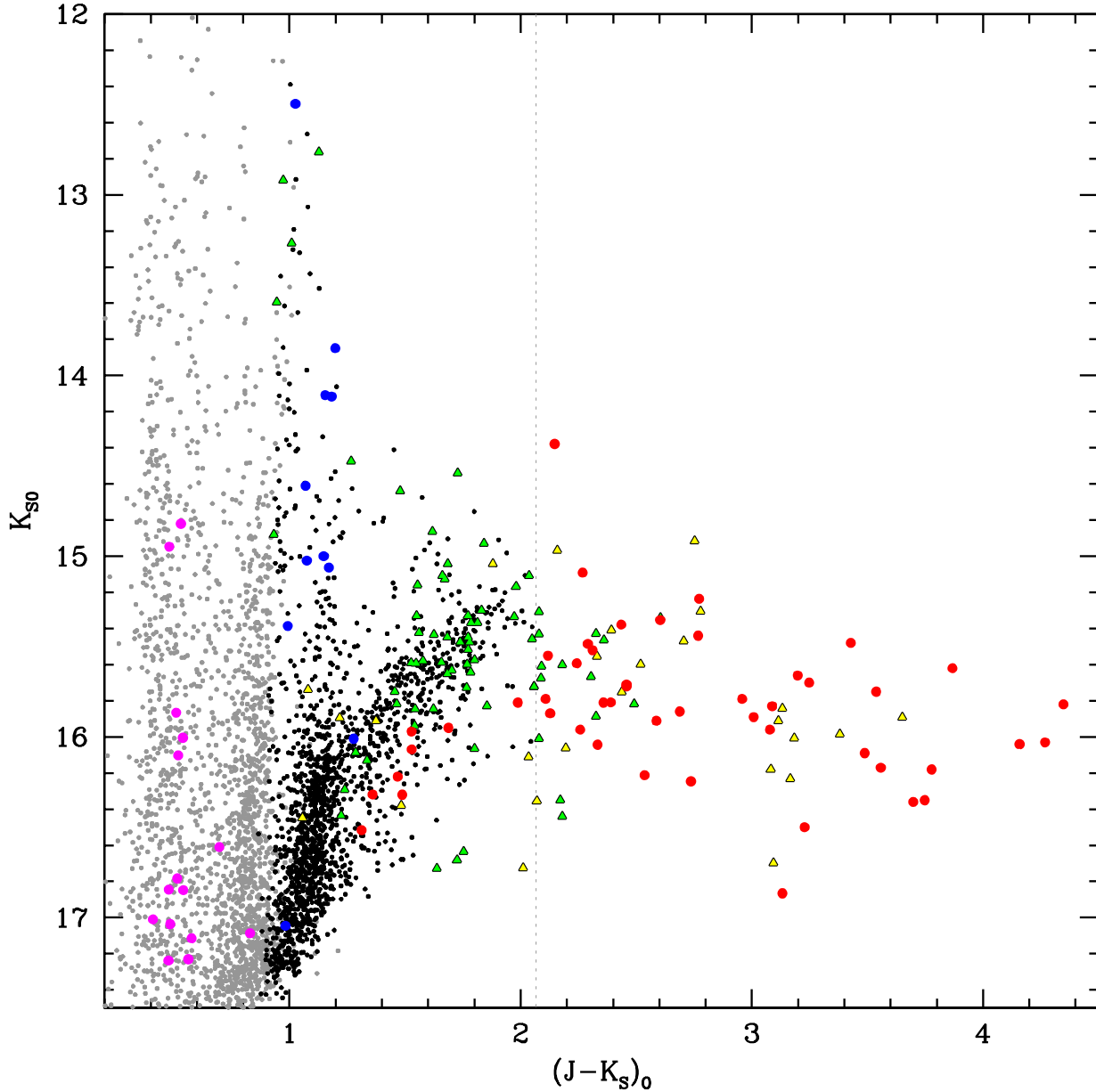


Figure 3. Colour-magnitude diagram illustrating the variable stars. Symbols: Cepheids magenta; M-type Miras and supergiant blue; C-type Miras red; other variables triangles: large amplitude yellow, small amplitude green. All stars to the right of the dotted line were systematically examined for variability.

mag) of the stars that we consider to be C stars in our PL relation analysis (see section 7 below).

Table 5 contains large amplitude (mostly $\Delta K_S > 0.4$ mag) but not obviously periodic variables; it includes some Miras for which we could not estimate periods and probably some unrecognized Miras (see below). Table 6 contains small amplitude ($\Delta K_S < 0.4$ mag) variables, most of which are not unambiguously periodic; these are probably semi-regular (SR) or irregular variables. This group includes a few which have SR-variations superimposed on an apparently secular

trend, which can make the overall change more than 0.4 mag. These are candidates for variables with two periods.

The distinction between Tables 5 and 6 is to some extent subjective and there is undoubtedly overlap between the two groups. Nevertheless, they do show distinctly different colours (see Figs. 3 and 4), with most of the large amplitude variables having larger values of $(J - K_S)$ than those with small amplitudes, suggesting that they have higher mass-loss rates.

Given the cadence of our observations and the fact that at least some mass-losing C-rich Miras undergo periods of

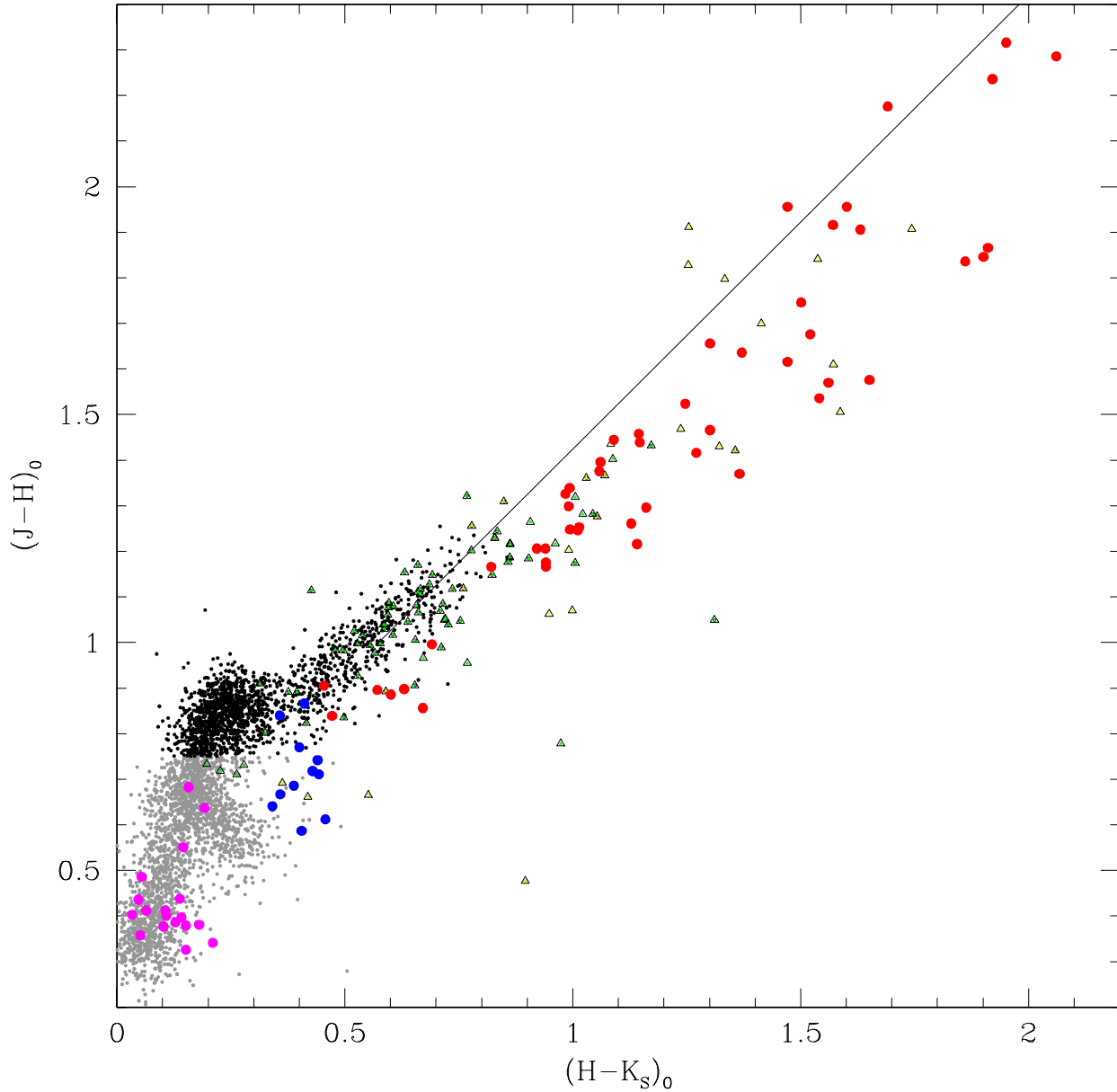


Figure 4. Two-colour diagram showing the same stars as in Fig. 3.

very erratic variation (e.g. R For as illustrated in Whitelock et al. (1997) and several LMC C-rich Miras discussed by Whitelock et al. (2003)) we anticipate that a significant fraction of the stars in Table 5 will be Miras of this type (see also N21029 in Fig. A2 in the appendix).

There are a few of the low amplitude variables among the supergiants. Note also that many of the AGB stars and supergiants not identified as variables will in fact be low amplitude variables, generally with $\Delta K_S < 0.2$ mag.

Table 4. (a) Periodic Large Amplitude O-Rich Variables (Miras). Fourier mean magnitudes \bar{J} , \bar{H} , \bar{K}_S are listed with the peak-to-peak amplitudes (ΔJ , ΔH , ΔK_S) of the best fitting first-order sine curves. The last column shows those with spectral types, or narrow band spectral indices (Letarte et al. 2002).

RA (2000.0)	Dec	N	P (days)	\bar{J}	\bar{H}	\bar{K}_S (mag)	ΔJ	ΔH	ΔK_S	Sp
296.18398	-14.78018	12557	158	18.23	17.51	17.12	0.84	0.83	0.80	M
296.25229	-14.78475	11226	257	17.49	16.54	16.08	0.54	0.58	0.53	M:
296.20415	-14.63486	20331	314	16.58	15.91	15.46	0.88	1.10	0.86	M
296.22364	-14.77473	10184	370	16.44	15.58	15.13	0.81	0.95	0.89	M
296.21816	-14.88035	30133	401	16.30	15.53	15.09	0.85	1.02	0.94	
296.21322	-14.68097	20134	402	16.35	15.55	15.07	0.89	1.00	0.92	
296.20428	-14.74271	40139	545	15.25	14.32	13.92	0.62	0.72	0.66	
296.25088	-14.76786	10198	602	15.50	14.68	14.19	0.75	0.93	0.80	
296.18801	-14.87231	30292	637	15.88	15.19	14.68	0.96	1.00	0.97	M
296.26702	-14.76311	10091	638	15.46	14.67	14.18	0.95	1.12	1.00	(1)
296.21293	-14.73224	20004	854	13.72	12.97	12.57	0.47	0.45	0.40	M

(1) N10091 was identified as a late-M star with H α emission by Filippenko & Chornock (2003).

Table 4. (b) Periodic Large Amplitude C-Rich Variables (Miras). Columns as given for Table 4a.

N	RA	Dec	P	\bar{J}	\bar{H}	\bar{K}_S	ΔJ	ΔH	ΔK_S	Sp
		(2000.0)	(days)			(mag)				
12790	296.20389	-14.75535	182	18.03	17.11	16.59	1.09	0.82	0.51	C6.5(1)
10817	296.23639	-14.83054	214	17.70	16.76	16.04	0.75	0.61	0.45	
20540	296.18011	-14.71067	223	17.88	16.89	16.39	0.94	0.71	0.48	C
40590	296.28567	-14.73952	223	18.01	17.04	16.39	0.80	0.63	0.39	C *
12751	296.21027	-14.75973	231	17.89	16.91	16.29	1.07	0.72	0.50	
11032	296.18048	-14.80431	239	18.20	16.91	15.94	1.20	0.92	0.65	
10748	296.17438	-14.83893	243	18.58	17.16	16.11	1.06	0.77	0.48	
20578	296.29065	-14.69641	246	17.80	16.82	16.14	0.77	0.79	0.43	C
20542	296.17703	-14.71031	255	17.84	16.76	16.02	0.73	0.66	0.50	C
30430	296.21802	-14.92573	269	17.67	16.56	15.86	0.87	0.63	0.38	C *
12208	296.23352	-14.80653	278	17.87	16.61	15.62	1.34	1.07	0.76	
21419	296.27563	-14.74923	278	19.93	18.27	16.57	1.50	1.42	1.05	
13364	296.19489	-14.82267	286	18.10	16.85	15.86	1.30	1.09	0.75	
12400	296.17468	-14.79389	301	18.00	16.75	15.88	1.11	0.84	0.60	C
30583	296.30014	-14.87872	302	18.37	17.07	15.88	1.2	1.1	0.5	C (4)
20239	296.22632	-14.72554	304	18.04	16.71	15.66	0.86	0.67	0.48	
20558	296.19647	-14.70265	304	18.21	16.60	15.31	0.41	0.40	0.44	(2)
20840	296.30347	-14.74166	306	18.7	17.18	15.98		1.14	0.88	(3)
12466	296.17462	-14.78854	311	18.42	17.09	16.03	1.52	1.17	0.96	
40114	296.19916	-14.86160	312	20.21	18.61	16.99	1.9	1.35	1.09	
11059	296.21259	-14.80142	319	18.38	16.90	15.79	1.20	1.01	0.75	
20375	296.18277	-14.74815	328	18.03	16.62	15.59	0.75	0.72	0.50	C
11296	296.21729	-14.77647	340	18.37	16.99	15.78	1.03	0.90	0.5	
30928	296.22229	-14.90997	342	18.95	17.42	16.28	0.57	0.62	0.48	
20657	296.22934	-14.65254	343	17.98	16.59	15.56	0.64	0.48	0.43	C8.2(1)
13106	296.24048	-14.84939	354	19.10	17.38	15.96	1.51	1.34	0.98	
20588	296.29919	-14.69143	376	17.56	16.22	15.16	0.97	0.80	0.57	C
11305	296.17957	-14.77527	378	18.02	16.56	15.45	0.82	0.63	0.50	
30920	296.24246	-14.91158	384	18.95	17.21	15.86	1.75	1.46	0.98	
40363	296.23649	-14.85697	398	19.18	17.73	16.32	1.00	0.91	0.85	C
11140	296.22876	-14.79337	405	18.75	17.25	15.93	0.91	0.95	0.83	
20439	296.24640	-14.73473	430	19.15	17.32	15.77	1.05	0.94	0.85	
10753	296.24295	-14.83836	432	18.40	17.06	15.88	0.66	0.75	0.76	
40520	296.26687	-14.74039	432	18.41	16.86	15.51	1.25	0.91	0.74	
31168	296.23883	-14.87026	434	19.49	17.50	15.82	2.05	1.40	1.01	
21671	296.26569	-14.72024	436	19.78	17.78	16.16	1.59	1.22	0.95	
11174	296.21774	-14.78943	440	19.12	17.42	15.90	1.31	1.24	0.89	
20569	296.29114	-14.69770	454	19.24	17.62	16.03	1.45	1.40	2.15	
12445	296.21661	-14.79057	454	20.26	18.34	16.43	2.42	1.78	1.25	
21141	296.29965	-14.69757	456	18.16	16.62	15.42	1.82	1.66	1.23	
21234	296.28125	-14.67393	466	20.16	18.21	16.25	1.54	1.41	1.25	
12147	296.28897	-14.81087	475	19.93	17.89	16.24	1.61	1.59	1.26	
11299	296.25732	-14.77645	494	19.06	17.30	15.73	2.16	2.07	1.67	
13293	296.25696	-14.83051	495	20.30	18.37	16.42	1.25	1.13	0.95	
21029	296.19858	-14.71837	501	19.11	17.07	15.55	1.5	1.1	0.8	(5)
40102	296.19682	-14.75119	526	19.69	17.43	15.69	2.12	1.31	1.05	
12177	296.28424	-14.80892	590	20.50	18.10	16.10	1.52	1.25	1.09	
10807	296.21631	-14.83196	747	20.37	18.00	15.89	1.92	2.13	1.59	
40623	296.29793	-14.74687	897	20.40	18.08	16.11	1.76	1.77	1.45	
30268	296.25891	-14.88796	998	16.73	15.44	14.45	1.35	1.47	1.21	

* Low K_S amplitude (< 0.4 mag) for a Mira.

(1) Spectral type from Kacharov et al. (2012).

(2) N20558 was not used in the PL analysis as its image appears blended.

(3) N20840 has only 4 good observations at J , therefore its mean is uncertain and its amplitude unknown.(4) N30583 has seven observations only; P taken from Battinelli and Demers (2011).

(5) N21029 has a long-term trend (see Fig. A2), mean given here for bright cycle.

Table 5. Large Amplitude Variables.

RA (2000.0)	Dec	N	J	δJ	H	δH (mag)	K_S	δK	$J - K_S$	NJ	NH	NK	note
296.29922	-14.83650	10293	17.87	0.88	16.35	0.72	14.98	0.07	2.88	16	17	8	
296.19168	-14.82965	10310	18.32	0.31	16.80	0.19	15.67	0.10	2.65	17	15	13	
296.28415	-14.81194	10371	17.33	0.16	15.94	0.12	15.04	0.07	2.29	15	14	12	
296.23456	-14.77330	10501	18.00	0.37	16.56	0.32	15.48	0.27	2.52	18	18	18	
296.20154	-14.81282	10968	19.18	0.60	17.30	0.30	15.91	0.20	3.27	18	18	18	
296.18323	-14.76308	11391	18.39	0.32	16.94	0.18	15.82	0.14	2.57	15	16	16	
296.27222	-14.76143	11401	18.09	0.24	16.73	0.17	15.62	0.07	2.46	17	18	13	
296.22778	-14.76111	11403	18.35	0.34	17.01	0.15	16.18	0.09	2.17	17	14	14	
296.27774	-14.82287	11991	18.46	0.18	17.17	0.22	16.13	0.20	2.33	18	18	18	
296.24905	-14.81619	12070	17.49	0.09	16.92	0.21	15.98	0.27	1.51	17	18	18	1
296.25348	-14.76936	12660	18.38	0.35	16.83	0.30	15.54	0.27	2.84	18	18	18	
296.24728	-14.76419	12711	18.94	1.05	17.79	0.92	16.80	0.63	2.14	18	18	17	
296.24246	-14.82114	13390	19.99	0.74	18.40	0.44	16.77	0.21	3.23	15	15	14	
296.17993	-14.75767	14105	19.23	0.39	17.44	0.33	15.98	0.26	3.25	17	16	16	
296.27051	-14.73481	20438	19.39	0.38	17.70	0.27	16.08	0.21	3.32	14	15	15	
296.18378	-14.68249	20608	19.57	1.40	17.64	0.95	16.06	0.67	3.51	15	17	17	
296.26770	-14.68061	20614	19.60	1.62	17.60	0.76	16.30	0.53	3.30	16	17	17	
296.17764	-14.64240	21316	18.63	0.79	17.47	0.64	16.42	0.45	2.20	15	17	17	
296.26511	-14.96155	30767	18.07	0.40	17.09	0.30	16.45	0.20	1.62	14	15	14	
296.21112	-14.91074	30924	19.46	0.36	17.55	0.20	16.25	0.13	3.21	13	14	12	
296.30179	-14.90356	30961	19.75	0.26	17.75	0.18	15.96	0.44	3.78	6	6	6	
296.18011	-14.75091	40030	17.02	0.16	16.27	0.20	15.81	0.12	1.21	23	30	29	
296.22681	-14.75065	40275	17.13	0.34	15.92	0.29	15.11	0.28	2.01	34	34	34	
296.23346	-14.74996	40327	17.71	0.18	16.93	0.23	16.52	0.18	1.19	31	35	33	
296.24622	-14.86655	40419	17.98	0.08	16.67	0.06	15.79	0.08	2.19	20	18	20	2
296.26105	-14.73764	40493	18.29	0.15	16.78	0.16	15.38	0.19	2.91	22	21	28	
296.27310	-14.75146	40538	17.31	0.16	16.57	0.17	15.96	0.20	1.35	29	30	31	

(1) N12070 is probably a Mira, with $\Delta K_S < 0.6$ mag, and possible periods of around 545 or 215 days, but its image is confused at shorter wavelengths.

(2) N40419 is a Mira with a period of 193 days, but its photometry is contaminated by nearby sources.

Table 6: Small Amplitude Variables.

RA (2000.0)	Dec	N	J	δJ	H	δH (mag)	K_S	δK	$J - K_S$	NJ	NH	NK
296.22696	-14.80191	10032	14.48	0.05	13.66	0.03	13.34	0.05	1.14	14	14	16
296.24005	-14.80796	10074	14.74	0.09	13.94	0.10	13.66	0.10	1.08	18	18	18
296.21835	-14.80118	10077	15.94	0.11	14.97	0.12	14.55	0.11	1.40	18	18	18
296.26028	-14.81812	10152	16.32	0.17	15.26	0.14	14.71	0.11	1.61	18	18	18
296.22321	-14.76671	10200	16.47	0.08	15.32	0.06	14.61	0.06	1.86	17	16	17
296.19437	-14.82407	10330	17.33	0.14	16.16	0.13	15.52	0.11	1.82	18	18	18
296.17441	-14.81870	10343	17.35	0.11	16.12	0.13	15.44	0.11	1.92	15	18	18
296.23013	-14.81558	10356	17.00	0.16	15.84	0.16	15.20	0.14	1.80	18	18	18
296.23392	-14.80649	10400	16.97	0.11	15.74	0.09	15.00	0.07	1.97	15	16	18
296.24081	-14.80368	10408	16.93	0.13	15.77	0.09	15.11	0.07	1.82	17	17	17
296.19797	-14.80259	10411	16.92	0.18	15.82	0.14	15.23	0.10	1.69	18	18	18
296.29706	-14.80268	10412	17.34	0.17	16.08	0.14	15.18	0.13	2.17	17	16	18
296.22131	-14.79940	10425	17.30	0.18	16.11	0.13	15.40	0.10	1.90	18	18	18
296.28729	-14.79597	10433	17.46	0.18	16.30	0.14	15.55	0.08	1.91	18	18	16
296.20374	-14.79388	10439	17.33	0.16	16.08	0.11	15.37	0.08	1.96	18	17	17
296.28287	-14.78797	10460	17.32	0.26	16.24	0.20	15.66	0.15	1.66	18	18	18
296.22369	-14.83960	10743	17.57	0.29	16.43	0.24	15.67	0.19	1.90	18	18	18
296.27734	-14.83831	10755	17.42	0.20	16.23	0.16	15.52	0.13	1.91	18	18	18
296.27213	-14.83158	10809	18.07	0.14	16.90	0.19	16.13	0.19	1.93	17	18	18
296.24747	-14.82692	10839	18.15	0.09	16.63	0.09	15.41	0.07	2.74	14	15	15
296.29504	-14.82570	10850	17.89	0.38	16.68	0.30	15.90	0.18	1.99	18	18	18
296.19476	-14.82463	10859	17.67	0.21	16.57	0.17	15.91	0.14	1.75	18	17	18
296.24554	-14.82244	10876	17.71	0.26	16.41	0.20	15.50	0.12	2.21	18	18	18
296.20242	-14.81780	10917	17.35	0.08	16.07	0.09	15.24	0.07	2.11	14	16	16
296.28149	-14.81671	10935	17.58	0.10	16.60	0.11	16.16	0.17	1.42	14	15	18
296.27066	-14.80596	11021	17.54	0.24	16.41	0.19	15.72	0.12	1.82	18	18	17
296.24573	-14.79360	11139	17.98	0.31	16.72	0.11	15.67	0.12	2.31	17	14	17
296.24271	-14.78809	11187	17.90	0.08	16.50	0.06	15.68	0.07	2.22	16	17	18
296.27832	-14.78018	11271	17.42	0.24	16.25	0.21	15.55	0.15	1.87	18	18	18
296.17908	-14.77972	11273	17.63	0.21	16.43	0.14	15.71	0.07	1.92	18	16	14
296.18372	-14.77252	11335	17.51	0.19	16.28	0.18	15.41	0.12	2.10	18	18	18
296.20221	-14.76910	11364	17.59	0.06	16.26	0.03	15.38	0.03	2.21	15	13	17
296.22644	-14.76749	11372	17.53	0.31	16.46	0.22	15.70	0.13	1.83	18	18	18
296.19781	-14.76344	11389	17.58	0.23	16.45	0.18	15.64	0.14	1.93	18	18	17
296.28235	-14.76346	11392	18.41	0.19	17.01	0.08	15.96	0.07	2.46	17	16	18
296.24139	-14.84622	11764	18.82	0.23	17.52	0.12	16.51	0.10	2.31	15	15	16
296.29608	-14.84267	11794	17.73	0.24	16.83	0.16	16.36	0.11	1.37	17	18	16

Continued on Next Page...

RA (2000.0)	Dec	N	J	δJ	H	δH (mag)	K_S	δK	$J - K_S$	NJ	NH	NK
296.24057	-14.79573	12373	18.57	0.32	17.52	0.24	16.80	0.09	1.77	16	17	13
296.18201	-14.78503	12496	18.17	0.28	16.81	0.25	15.74	0.22	2.44	17	18	18
296.25473	-14.75607	12784	18.51	0.22	17.03	0.17	15.89	0.11	2.62	18	18	17
296.20816	-14.72616	20022	14.09	0.09	13.21	0.08	12.83	0.08	1.26	16	16	17
296.26938	-14.66636	20311	17.19	0.12	16.20	0.16	15.49	0.07	1.69	14	17	14
296.23389	-14.72910	20463	17.86	0.16	16.87	0.09	16.51	0.14	1.36	11	13	13
296.29358	-14.72387	20496	17.36	0.20	16.28	0.17	15.65	0.13	1.71	16	17	17
296.17297	-14.71139	20539	17.96	0.22	16.59	0.19	15.50	0.10	2.46	13	17	15
296.26337	-14.70901	20547	17.34	0.09	16.23	0.09	15.66	0.08	1.68	15	16	17
296.24963	-14.71943	21021	18.72	0.09	17.38	0.05	16.42	0.06	2.30	14	15	16
296.28815	-14.67794	21217	17.67	0.16	16.75	0.13	16.20	0.13	1.47	15	16	16
296.25790	-14.90380	30244	17.38	0.14	16.17	0.12	15.44	0.10	1.95	14	15	14
296.20166	-14.88640	30271	16.68	0.11	15.57	0.10	14.93	0.08	1.75	13	14	14
296.28564	-14.87809	30285	16.97	0.16	15.88	0.13	15.18	0.04	1.79	14	15	10
296.20511	-14.87565	30590	17.68	0.28	16.48	0.05	16.01	0.12	1.67	14	10	14
296.19254	-14.86788	30611	18.29	0.26	16.99	0.20	16.08	0.13	2.21	14	15	14
296.29318	-14.90858	30934	18.03	0.09	16.89	0.05	15.53	0.04	2.49	14	13	11
296.17282	-14.75015	40002	17.59	0.11	16.53	0.06	15.91	0.04	1.68	26	26	24
296.17505	-14.85986	40007	17.97	0.11	16.70	0.12	15.75	0.04	2.22	24	30	22
296.17966	-14.73710	40026	17.49	0.19	16.36	0.15	15.59	0.10	1.90	16	31	27
296.20724	-14.74512	40155	17.08	0.09	16.00	0.06	15.40	0.05	1.68	34	35	29
296.22379	-14.73659	40257	16.01	0.02	15.20	0.05	14.95	0.03	1.06	18	21	17
296.22452	-14.86319	40261	17.48	0.17	16.42	0.12	15.89	0.10	1.60	30	30	29
296.24301	-14.74652	40397	14.10	0.07	13.30	0.06	12.99	0.07	1.11	34	36	36
296.24622	-14.86655	40419	17.98	0.08	16.67	0.06	15.79	0.08	2.19	20	18	20
296.24634	-14.86488	40421	17.41	0.06	16.40	0.05	15.82	0.04	1.59	25	24	21
296.25229	-14.74336	40445	17.70	0.18	16.57	0.18	15.80	0.08	1.90	31	35	29
296.25253	-14.86060	40446	18.61	0.41	17.57	0.43	16.75	0.31	1.86	33	33	29
296.25864	-14.73680	40476	17.71	0.08	16.44	0.05	15.53	0.03	2.18	29	25	23
296.25992	-14.74793	40486	18.59	0.17	17.73	0.29	16.70	0.13	1.88	26	33	25
296.26254	-14.84794	40501	17.26	0.14	16.14	0.09	15.51	0.11	1.76	29	25	28
296.27545	-14.85393	40547	17.45	0.17	16.30	0.10	15.66	0.10	1.79	26	25	32

5.1 Comparison with Battinelli and Demers (2011)

Battinelli & Demers (2011) discuss long period variables discovered in their 32 arcmin square survey of NGC 6822 using 1.5-m and 1.6-m telescopes, over a period of somewhat over three years. There is considerable overlap with our work although their survey extends further to the east (they also have unpublished data extending to the west). Twenty of their variables fall within the area we surveyed.

Table 7 lists 16 of those 20 variables that we also regard as large amplitude variables and for which we derived periods. It includes the long period Cepheid, our N10170. The other 4 are briefly described below:

BD v13, for which they find a period of 466 days, corresponds to our N20438 (Table 5) and its K light curve is illustrated in Fig. 6. Although it shows large amplitude variations its behaviour was not sufficiently regular for us to identify it as periodic, and it is therefore included in Table 5. However, knowing the period and examining the light curve it is possible to see that it underwent two maxima during the time we observed it, the first at $K_S \sim 15.8$ mag and the second at $K_S \sim 15.3$ mag.

BD v14 is N40538 and is also a variable (Table 6), but without a clearly defined period.

BD v9 is N20287 which is not obviously significantly variable.

BD v21 was very faint on the H frame that we used as a reference, and was therefore not extracted in our survey, although it is clearly seen on the K frames. Battinelli & Demers determined $P=613$ days and $\Delta K_S = 0.7$ mag for this star.

All of the other variables from Battinelli & Demers's table 3 are outside the positional range of our survey. Fig. 5 compares their periods and mean K_S magnitudes with ours for the stars in common. We note that while the periods are in reasonable agreement there does appear to be a systematic difference in the mean K_S magnitude. The mean difference is 0.25 mag, or 0.21 mag leaving out BD v19=N21141 where the mean magnitudes differed by 0.8 mag. It is disturbing to find such a large difference in the magnitudes of potential distance indicators and the matter is worth further investigation. There are no non-variable stars in Battinelli & Demers to compare with ours, but we have made the comparison with the UKIRT photometry of Sibbons et al. (2012). The difference between their K_S magnitudes and ours, both uncorrected for interstellar reddening, is only 0.05 mag at $K_S = 16$ mag and about 0.1 mag at $K_S = 17$ mag. At the fainter magnitudes crowding can be a problem for matching objects between the two catalogues, quite apart from possible photometric difficulties. Neither study has taken account of any possible colour equation, both being essentially on the natural system. Though colour effects are probably not significant if $J - K_S < 1.0$ mag, they may need to be considered for the reddest stars considered here, but it is extremely difficult to do the calibration work required to quantify the effect.

Given that our entire field falls within the area discussed by Battinelli & Demers it is a little surprising that they do not find more of the Mira variables that we identify. Six more of them are to be found in their table 4 which lists SR and irregular variables and Table 8 cross references our

Table 7. Variables in common with Battinelli & Demers (2011) table 3

N	P (days)	K_S (mag)	BD	P (days)	K_S (mag)
40102	526	15.69	1	576	15.80
40114	312	16.99	2	339	17.25
20331	314	15.46	3	326	15.67
20134	402	15.07	4	403	15.14
10807	747	15.89	5	777	16.25
12445	454	16.43	6	437	16.32
31168	434	15.82	7	447	16.20
10198	602	14.19	8	673	14.25
10170	123	14.92	10	124	14.80
30268	998	14.45	11	992	14.85
40520	432	15.51	12	436	15.75
12177	590	16.10	15	633	16.25
40590	221	16.39	16	223	16.80
40623	897	16.11	17	1100	16.60
21141	456	15.42	19	448	16.25
30583	305:	15.55	20	302	15.85

Table 8. Variables in common with Battinelli & Demers (2011) table 4

BD	N	remark
100	30981	
101	11173	
102	11296	Mira Table 4
103	11414	
104	20468	
105	20239	Mira Table 4
106	11372	
107	10501	LPV trend Table 5
108	30920	Mira Table 4
111	20892	
112	12660	LPV trend Table 5
113	11299	Mira Table 4
114	11362	
115	40482	
116	40520	=ID12 Mira Table 4
118	20569	Mira Table 4
119	20588	Mira Table 4

identification numbers with theirs (note that their BD v116 has the identical coordinates to their BD v12). They do not appear to have found the other 39.

Among their SR variables BD v109 is not measurable on our image where it is extended, while BD v117 is another very red object, visible at K_S but not at shorter wavelengths. The other variables they list are outside of our survey area.

5.2 M-type Miras

The most luminous of the stars in Table 4(a), N20004, is a known variable, NGC6822 V12. Kayser (1967) describes this as a semi-regular and writes 'Most of the time it varies regularly with a period of 640 days, but every three to six cycles it does something else for 180 days'. Note that 640 days

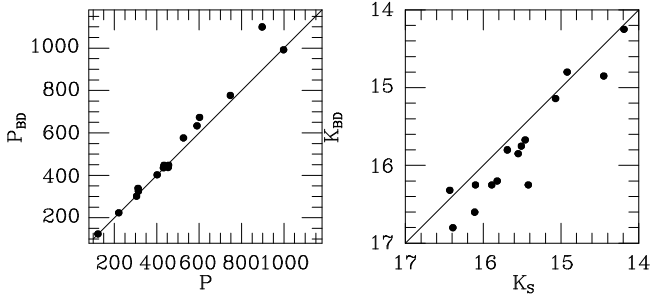


Figure 5. A comparison of the periods and mean K magnitudes derived here and by Battinelli & Demers (2011).

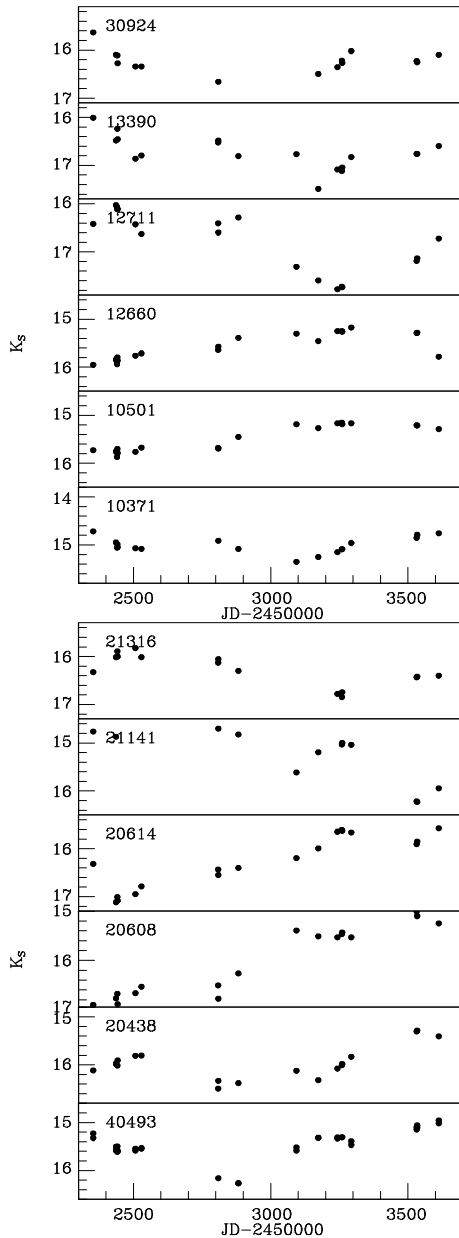


Figure 6. The light-curves for some of the large amplitude variables without obvious periodicity.

v

Table 9. Bolometric magnitudes of the assumed O-rich Miras.

N	P (days)	m_{bol}	$(J - K_S)_0$ (mag)
12557	158	20.13	1.05
11226	257	19.27	1.37
20331	314	18.51	1.06
10184	370	18.27	1.25
30133	401	18.19	1.15
20134	402	18.21	1.23
40139	545	17.05	1.28
10198	602	17.36	1.27
30292	637	17.80	1.15
10091	638	17.34	1.24
20004	854	15.62	1.10

is significantly different from the 854 days that we found. Massey (1998) gives its spectral type as M2.5-3I: and JHK photometry was published by Elias & Frogel (1985). Its amplitude is lower, and luminosity higher, than those of the other variables considered here and it is possibly the descendent of a more massive star and different from the other O-rich variables, but that is not entirely clear. Its luminosity is comparable to the supergiants discussed by Levesque & Massey (2012).

N10198 was identified as a variable, v198, by Baldacci et al. (2005). N10184 and N11226 were identified as variables, v1838 and v1534, respectively, by Antonello et al. (2002). N40139 appears in the GCVS as v16.

The bolometric magnitudes of the presumed O-rich stars were calculated by fitting a blackbody to the JHK fluxes, following the procedure used by Robertson & Feast (1981) and by Feast et al. (1989). In practice, for these stars with very thin shells, bolometric magnitudes derived in this way differ insignificantly (< 0.03 mag) from those calculated using the bolometric corrections defined for the C stars (section 7). The results are listed in Table 9 and illustrated in a PL relation (Fig. 7).

The two short period stars are presumably similar to the short period O-rich Miras found in globular clusters (Feast et al. 2002; Whitelock et al. 2008), and their luminosities are comparable to those of the short period C-rich Miras. The brighter, longer period, stars appear to represent a somewhat younger population. They are probably similar to long-period O-rich Miras that are found in the LMC, many of which have s-process enhancements (Lundgren 1988; Smith et al. 1995). They are considered further in the next section.

5.3 C-type Miras

These are discussed below in section 7.

6 COMPLETENESS OF LARGE AMPLITUDE VARIABLE SURVEY

We measured pulsation periods for 61 Mira variables in our survey area, compared to the 20 measured by Battinelli & Demers (2011) in the same area (only 16 of these are in common). So there is no question that we significantly improved

Table 10. Bolometric magnitudes of the assumed C-rich Miras.

N	P (days)	m_{bol}	$(J - K_S)_0$ (mag)
12790	182	19.82	1.34
10817	214	19.41	1.56
20540	223	19.63	1.39
40590	223	19.74	1.52
12751	231	19.62	1.50
11032	239	19.34	2.16
10748	243	19.48	2.36
20578	246	19.50	1.56
20542	255	19.42	1.72
11226	257	19.27	1.31
30430	269	19.25	1.71
12208	278	19.02	2.15
21419	278	19.29	3.26
13364	286	19.26	2.14
12400	301	19.30	2.02
30583	302	19.19	2.39
20558	304	18.47	2.80
20239	304	19.04	2.27
20840	306	19.24	2.62
12466	311	19.40	2.29
20331	314	18.51	1.02
40114	316	19.76	3.16
11059	319	19.11	2.49
20375	328	18.96	2.34
11296	340	19.06	2.49
30928	342	19.58	2.57
20657	343	18.93	2.32
13106	354	18.98	3.04
10184	370	18.27	1.20
20588	376	18.53	2.30
11305	378	18.78	2.47
30920	384	18.94	2.99
40363	398	19.41	2.77
30133	401	18.18	1.11
20134	402	18.22	1.18
11140	405	19.10	2.72
20439	430	18.61	3.28
40520	432	18.64	2.80
10753	432	19.19	2.42
31168	434	18.44	3.57
21671	436	18.85	3.52
11174	440	18.82	3.12
12445	454	18.76	3.73
20569	454	18.89	3.11
21141	456	18.68	2.64
21234	466	18.50	3.81
12147	475	18.88	3.59
11299	494	18.57	3.23
13293	495	18.69	3.78
21029	501	18.34	3.46
40102	526	18.11	3.90
40139	545	17.03	1.23
12177	590	18.08	4.30
10198	602	17.36	1.21
30292	637	17.81	1.10
10091	638	17.34	1.19
10807	747	17.71	4.38
20004	854	15.60	1.06
40623	897	18.07	4.39
30268	998	17.84	2.18

on their count. However, we note that our survey will still be incomplete for the following reasons:

(1) We may have missed a very small number of very red, dust enshrouded, large amplitude variables entirely (see section 5.1) and indeed we did miss one of those found by Battinelli & Demers. Nevertheless it is interesting to see that we have one assumed C-rich Mira, with a period of 998 days (N30268 for which there is no measured spectral type).

It has been suggested that at periods longer than about 1000 days the stars are sufficiently massive for hot bottom burning to occur and that will result in O-, rather than C-rich Miras (Feast 2009). The longest period C-rich Miras in the LMC are also just under 1000 days (Whitelock et al. 2003). It would obviously be very interesting to know if we have any OH/IR stars in NGC 6822 with periods over 1000 days.

(2) Some Miras behave erratically and very long-term monitoring is necessary to characterize them. That is one of the reasons for differences with Battinelli & Demers. Most such stars will appear in Tables 5 or 6.

(3) Confusion, especially in the crowded inner regions, limits our ability to measure the Miras, particularly at J .

All of these factors are relevant, but the only one that is likely to seriously affect the total count is item (2).

7 PERIOD-LUMINOSITY RELATIONS

There are a variety of ways in which bolometric magnitudes can be measured or estimated, depending on the information available and, to some extent, on the desired objective. Given that one is almost always limited by temporal and/or spectral coverage any chosen approach is a compromise. Kerschbaum, Lebzelter & Makul (2010) discuss different approaches and show that they can lead to very different results: over 0.5 mag spread at a particular colour. We also note that Kamath et al. (2010) and Groenewegen et al. (2007) derive bolometric magnitudes for several variable stars in the SMC cluster NGC 419 using the same Spitzer data and slightly different $JHKL$ values. Their bolometric magnitudes differ by amounts that range from -0.1 to 0.4 mag for the same star.

These uncertainties present difficulties when attempting to compare bolometric luminosities with theoretical predictions. For instance, in a plot of bolometric magnitude against period (their fig. 7), Kamath et al. place a group of NGC 419 carbon-rich semi-regular variables on their computed fundamental sequence and a group of brighter shorter period variables on their first overtone sequence. This is contrary to the usually accepted model of the overall evolution that increasing luminosity and period implies decreasing mode. Such a normal evolutionary sequence is supported by the $K - \log P$ plot for these same NGC 419 variables. This places them all together in a single group on the first overtone sequence in a “Wood” PL diagram (for instance the LMC/SMC plots of Ita et al. 2004).

For the purpose of this paper we follow the same procedure for determining bolometric magnitudes as in our previous papers as this will give us consistent values that are good, at least, for estimating distances via the PL relation.

Bolometric magnitudes for the presumed C stars were calculated in the same way as in our earlier papers (e.g.

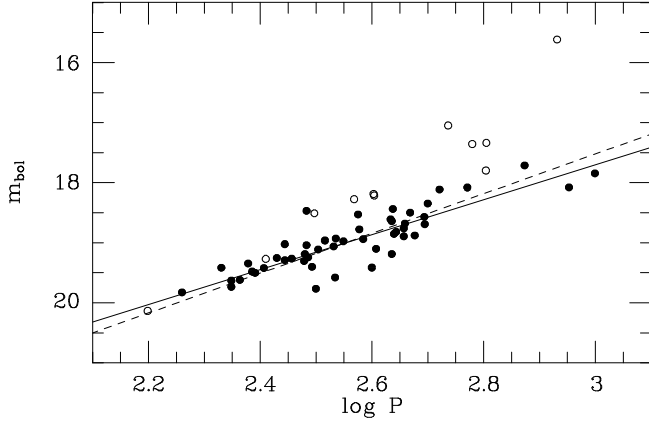


Figure 7. Bolometric PL for the large amplitude variables in NGC 6822; open symbols are those from Table 4(a); closed symbols represent those from Table 4(b). The solid line is the best fit to the closed circles while the dashed line is the best fitting one with the same slope as the LMC PL relation.

Whitelock et al. 2009), by applying a colour-dependent bolometric correction to the reddening-corrected K magnitudes on the SAAO system. The magnitudes given in Table 4, which are on the 2MASS system, are converted to the SAAO system following Carpenter (2001 and web page update²). The resulting bolometric magnitudes are listed in Table 10.

Note that the bolometric magnitudes derived for stars with faint J magnitudes are rather uncertain due to photometric errors and the increased possibility of confusion.

Figure 7 shows a PL relation. A least squares fit to the 50 presumed C-rich Miras gives the following result:

$$m_{bol} = 19.16(\pm 0.04) - 2.91(\pm 0.22)[\log P - 2.5], \quad (1)$$

with a scatter of 0.23 mag. This expression is shown as a solid line in Fig. 7.

Alternatively, if we assume that the slope of the PL relation is the same as that found in the LMC, -3.31 ± 0.24 (Whitelock et al. 2009), then we derive a zero point of 19.18 ± 0.03 , with a scatter of 0.24 mag for the same 50 stars. This line is also shown in Fig. 7.

If we restrict the stars in NGC 6822 to cover the same range of periods as used to derive the LMC PL relation, i.e. $220 < P < 500$, then the zero-point is 19.20 ± 0.04 , with a scatter of 0.23 mag for 41 stars.

Leaving out the stars with the faintest J magnitudes, $J > 20.0$ mag, which have the most uncertain bolometric magnitudes, we find a zero point of 19.16 ± 0.04 , with a scatter of 0.22 mag for 40 stars.

Leaving out only star N40114, which is unusually red ($J - K \sim 3.28$) for a $P=313$ day Mira and rather faint with respect to the PL relation, gives a zero point of 19.17 ± 0.03 , with a scatter of 0.22 mag for 49 stars

Thus these results are consistent with the PL relation in NGC 6822 having the same slope as it does for the LMC. If we assume that the distance of the LMC is $(m - M)_0 = 18.50$ mag, the PL relation derived from LMC Miras is

$$M_{bol} = -4.38 - 3.31[\log P - 2.5],$$

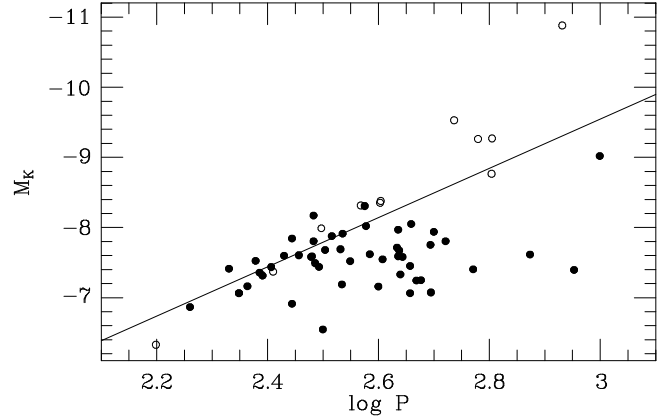


Figure 8. PL(K) for the large amplitude variables in NGC 6822; symbols as in Fig. 7. The solid line is the PL(K) derived for the Galactic O-rich Miras assuming $(m - M)_{LMC} = 18.5$ mag. The absolute K magnitudes shown here assumes $(m - M)_{NGC6822} = 23.38$ mag, as was determined from the 4 faintest O-rich Miras.

and using the zero point of 19.18 ± 0.03 , the distance modulus for NGC 6822 is $(m - M)_0 = 23.56(\pm 0.03)$ mag. The uncertainty does not include the uncertainty on the LMC distance. This can be compared with values of 23.40 mag and 23.49 derived from Cepheids and RR Lyraes, respectively (Feast et al. 2012; Clementini et al. 2003).

In the PL(K) diagram (Fig. 8) many of the C-rich Miras fall below the anticipated PL relation, because circumstellar extinction is sufficiently strong to affect their K magnitudes, in some cases by more than one magnitude. This is illustrated by Nsengiyumva (2010 his fig. 3.9) in a plot of the difference between K observed and predicted from the PL relation, as a function of $J - K$ colour.

The O-rich Miras fall in approximately the same region as do the C-rich ones at shorter periods, but above $\log P > 2.7$ they are consistently brighter than the PL relation. These are the same stars that fall to the upper left of the C stars in the colour-magnitude diagram (Fig. 3). The same is found for Miras in the LMC as discussed by Whitelock et al. (2003), who suggested that the high luminosity of these O-rich stars was a consequence of hot bottom burning, which is expected for intermediate mass AGB stars. Feast (2009) has suggested that their position in the PL relation is consistent with their being overtone pulsators, which may eventually evolve into long period OH/IR stars.

In view of the fact that these O-rich Miras do not have significant circumstellar reddening we can use the PL(K) relation derived by Whitelock et al. (2008) to derive a distance. For this we use only the four stars with $P < 400$ days, as longer period O-rich Miras are usually brighter than the PL(K) would predict. We use the relation derived for Galactic stars by Whitelock et al. (2008):

$$M_K = 3.51[\log P - 2.38] - 7.37,$$

which assumes the same LMC distance as above. Transforming the 4 K magnitudes onto the SAAO system as before gives a distance modulus for NGC 6822 of 23.38 ± 0.16 mag.

Given the uncertainties, including the fact that the LMC distance may vary with the sample of LMC stars studied (e.g. Feast et al. 2012), the various estimates of the NGC 6822 distance modulus are not in conflict.

² <http://www.astro.caltech.edu/jmc/2mass/v3/transformations/>

8 COMPARISON WITH THE DWARF SPHEROIDALS

It is instructive to compare what we find here with the period distribution of Miras in other Local Group galaxies and in particular with those in the dwarf spheroidals that were surveyed in the same way. Figure 9 shows a histogram of the periods for the presumed C-rich Mira variables and compares them with those found in the dwarf spheroidals. The following dwarf spheroidals are involved (Mira periods, in days, given in parenthesis after the names): Sculptor (189, 554, Menzies et al. 2011), Fornax (215, 258, 267, 280, 350, 400, 470, Whitelock et al. 2009), Phoenix (425 Menzies et al. 2008), Leo I (158, 180, 191, 252, 283, 336, 523, Menzies et al. 2010) and Leo II (183 unpublished). We include the Phoenix dwarf galaxy with this group, but note that it is generally classed as intermediate between dwarf irregular and dwarf spheroidal (e.g. Battaglia et al. 2012).

Figure 9 also shows the period distribution of probable C-rich Miras in the LMC taken from Soszyński et al. (2009), which is based on the OGLE III catalogue. Care is required in comparing frequency distributions of AGB variables derived from surveys with different sensitivities and in different wavelength regions (OGLE III is a V and I survey), because the different selection effects will affect the colour- and period-range of the variables found. In particular longer wavelength surveys tend to find larger numbers of redder and longer period variables.

The distribution of large amplitude carbon variables with period found for NGC 6822 is similar to that shown by carbon AGB variables in both the LMC and SMC (see Soszyński et al. 2011 fig. 3 for the SMC). It is also clear that there are very few short period carbon variables on the Wood sequence C (the Mira sequence) of any amplitude in either Magellanic Cloud. It is notable that the distribution of LMC and SMC C-rich variables in both the amplitude-period and the PL relations appear to be very similar though the ratio of O-rich to C-rich variables differs greatly.

While the existence of Miras with periods in excess of 600 days in NGC 6822 is quite striking, they only constitute 6 percent of the total number. Thus we would only expect to see one in all the Local Group dwarf spheroidals if they were present in the same proportions. However, our survey is probably not complete for long-period variables, as our failure to identify BD v21 ($P=613$ days) shows; it was too faint at H .

The smaller fraction of short period Miras, less than 300 days, in NGC 6822 and the Magellanic Clouds compared to the dwarf spheroidals, is notable. Of course for short period Miras the magnitudes are fainter and the amplitudes are lower (on average) than they are for the longer period stars, so they are more difficult to find. Nevertheless, we have followed the same procedure here as we did in the dwarf spheroidals to identify variables, so we should have found them if they were there, provided that they did not have exceptional dust shells. For example, BD v16 (our N40590) was not initially identified as a Mira by us, presumably because its amplitude was slightly lower when we observed it than when they did. It seems that the variables in NGC 6822 with periods less than 300 days have low amplitudes, i.e., there are no stars like L7020 in Leo I which has $\Delta K_S = 1.2$ mag and $P = 191$ days. However, L2077 in Leo I which has

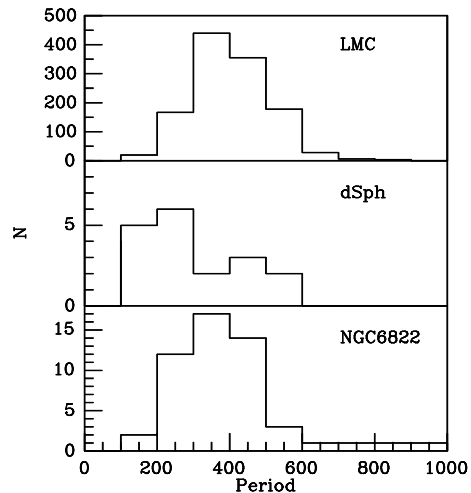


Figure 9. Histogram of the periods of the C-rich Miras in NGC 6822 (lower panel including N40419 $P=193$ days and BD v24 $P=670$ days) and in the four dwarf spheroidals (central panel) and LMC (top panel from Soszyński et al. (2009)).

$\Delta K_S = 1.2$ mag and $P = 283$ days is much redder with mean magnitudes of $J = 20.9$, $H = 19.0$ and $K_S = 17.4$. Given that our sensitivity is limited to stars with $H < 18.3$ mag this star would have been missed.

Since the period decreases with increasing age for Miras, it seems probable that the different period distributions are due to a larger proportion of an older C-rich population in the dwarf spheroidals. The evolutionary status of this population is somewhat problematic, as discussed by Menzies et al (2011).

Although we have spectral types for only a few of the Miras in any of these galaxies, the dwarf spheroidals do not have any long period M stars that we know of. This of course is to be expected given what we know about the metallicity and star formation history of the dwarf spheroidals.

9 CONCLUSIONS

The large number of C-rich Miras now found in NGC 6822 allows us to demonstrate that the slope of the bolometric PL relation in that galaxy is, within the errors, the same as that in the LMC. The distance modulus found from this relation is in satisfactory agreement with that found by other methods and with that derived from the PL(K) relation for the small number of shorter period O-rich Miras. Whilst there are problems with determining bolometric magnitudes for C-rich AGB stars, these are not important for distance scale studies provided a consistent method is employed for both programme stars and calibrators. The period distribution of high amplitude carbon-rich AGB variables in NGC 6822 is probably similar to that in the two Magellanic Clouds but differs from that in Local Group dwarf spheroidals, which contain a population of high amplitude, short period C-rich variables. Since these short period stars are believed to be old, this indicates that the dwarf spheroidals contain an old population that is capable of producing C-rich AGB variables which is absent or

relatively rare in both NGC 6822 and the Magellanic Clouds.

ACKNOWLEDGEMENTS

This publication makes extensive use of the various databases operated by CDS, Strasbourg, France. MWF, JWM and PAW gratefully acknowledge the receipt of research grants from the National Research Foundation (NRF) of South Africa and FN thanks the National Astrophysics and Space Science Programme (NASSP) of South Africa for financial support. We would also like to thank Serge Demers for sending us data and preprints of his work with Paolo Battinelli in advance of publication and the referee Jacco van Loon for his comments.

REFERENCES

- Aaronson M., Mould J., Cook K. H., 1985, *ApJ*, 291, L41
 Antonello E., Fuazza D., Mantegazza L., Stefanon M., 2002, *IBVS*, 5251, 1
 Baldacci L., Rizzi L., Clementini G., Held E. V., 2005, *A&A*, 431, 1189
 Battaglia G., Rejkuba M., Tolstoy E., Irwin M. J., Beccari, G., 2012, *MNRAS*, 424, 1113
 Battinelli P., Demers S., 2011, *A&A*, 525, 69
 Carpenter J.M., 2001, *AJ*, 121, 2851
 Cannon J.M., et al., 2012, *ApJ*, 747, 122
 Cioni M.-R. L., Habing H. L., 2005, *A&A*, 429, 837
 Clementini G., Held E.V., Baldacci L., Rizzi L., 2003, *ApJ*, 588, L85
 Demers S., Battinelli P., Kunkel W., 2006, *ApJ*, 636, L85
 Elias J. H., Frogel J. A., 1985, *ApJ*, 289, 141
 Feast M. W., 2009, in: Ueta, Matsunaga, Ita, (eds.) *AGB Stars and Related Phenomena*, a conference in honour of Y. Nakada, p. 48
 Feast M. W., Glass I. S., Whitelock P. A., Catchpole R. M., 1989, *MNRAS*, 241, 375
 Feast M. W., Whitelock P. A., Menzies J. W., 2002, *MNRAS*, 329, L7
 Feast M. W., Whitelock P. A., Menzies J. W., Matsunaga N., 2012, *MNRAS*, 421, 2998
 Filippenko A. V., Chornock R., 2003, *IAUC* 8158
 Groenewegen M. A. T. et al., 2007, *MNRAS*, 376, 313
 Groenewegen M. A. T., Lançon A., Marescaux M., 2009, *A&A*, 504, 103
 Ita Y., et al., 2004, *MNRAS*, 347, 720
 Kacharov N., Rejkuba M., Cioni M.-R. L., 2012, *A&A*, 537, A108
 Kang A., Sohn Y.-J., Kim H.-I. et al., 2006, *A&A*, 454, 717
 Kamath D., Wood P. R., Soszyński I., Lebzelter T., 2010, *MNRAS*, 408, 522
 Kayser S. E., 1967, *AJ*, 72, 134
 Kerschbaum F., Lebzelter T., Makul L., 2010, *A&A*, 524, A87
 Kniazev A. Y., et al., 2009, *MNRAS*, 395, 1121
 Levesque E. M., Massey P., 2012, *AJ*, 144, 2
 Letarte B., Demers S., Battinelli P., Kunkel W. E., 2002, *AJ*, 123, 832
 Lundgren K., 1988, *A&A*, 200, 85
 Massey P., 1998, *ApJ*, 501, 153
 Menzies J., Feast M., Tanabé T., Whitelock P., Nakada Y., *MNRAS*, 2002, 335, 923
 Menzies J., Feast M., Whitelock P., Olivier E., Matsunaga N., da Costa G., 2008, *MNRAS*, 385, 1045
 Menzies J., Whitelock P., Feast M., Matsunaga N., 2010, *MNRAS*, 406, 86
 Menzies J., Feast M., Whitelock P., Matsunaga N., 2011, *MNRAS*, 414, 3492
 Muschelok B., Kudritzki R. P., Appenzeller, I. et al. 1999, *A&A*, 352, 40
 Nagayama T., et al., 2003, *SPIE*, 4841, 459
 Nikolaev S., Weinberg M. D., 2000, *ApJ*, 542, 804
 Nsengiyumva F., 2010, *Asymptotic Giant Branch Variables in NGC 6822*, MSc thesis, University of Cape Town
 Persson S.E., Madore B.F., Krzemiński W., Freedman W.L., Roth M., Murphy D.C., 2004, *AJ*, 128, 2239
 Robertson B. S. C., Feast M. W., 1981, *MNRAS*, 196, 111
 Sackmann I.-J., Boothroyd A., 1992, *ApJ*, 392, L71
 Schlegel D.J., Finkbeiner D.P., Davis M., 1998, *ApJ*, 500, 525
 Siess L., 2008, in: Deng, L., & Chan, K.L. (eds.), *The Art of Modeling Stars in the 21st Century*, *IAUS*, 252, 297
 Sibbons L. F., Ryan S. G., Cioni M.-R. L., Irwin, M., Napiwotzki R., 2012, *A&A*, 540, 135
 Smith V. V., Plez B., Lambert D. L., Lubowich D. A., 1995, *ApJ*, 441, 735
 Soszyński I. et al. 2009, *Act.Ast.*, 59, 239
 Soszyński I. et al. 2011, *Act.Ast.*, 61, 217
 Whitelock P. A., 1997, in: R. Ferlet, J.-P. Maillard, B. Raban (eds.) *Variable Stars and the Astrophysical Returns of Microlensing Surveys*, Editions *Frontieres*, p. 163
 Whitelock P. A., Feast M. W., Marang F., Overbeek M. D., 1997, *MNRAS*, 288, 512
 Venn K.A. et al., 2001, *ApJ*, 547, 765
 Whitelock P. A., Feast M. W., van Loon J. Th., Zijlstra A. A., 2003, *MNRAS*, 342, 86
 Whitelock P. A., Feast M. W., Marang F., Groenewegen M. A. T., 2006, *MNRAS*, 369, 751
 Whitelock P. A., Feast M. W., van Leeuwen F., 2008, *MNRAS*, 386, 313
 Whitelock P. A., Menzies J. W., Feast M. W., Matsunaga N., Tanabé T., Ita Y., 2009, *MNRAS*, 394, 795
 Wood P. R., 2000, *PASA*, 17,18

APPENDIX

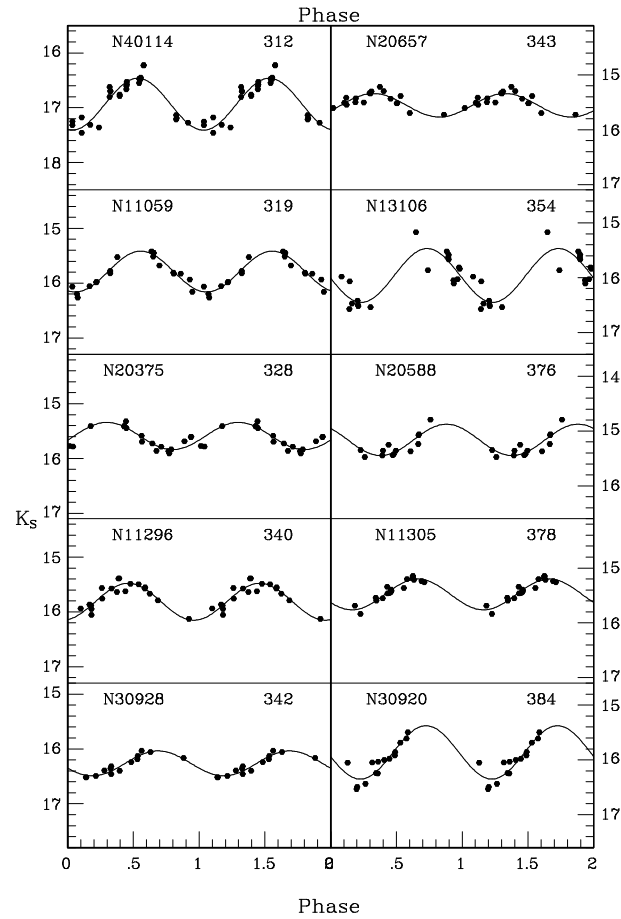
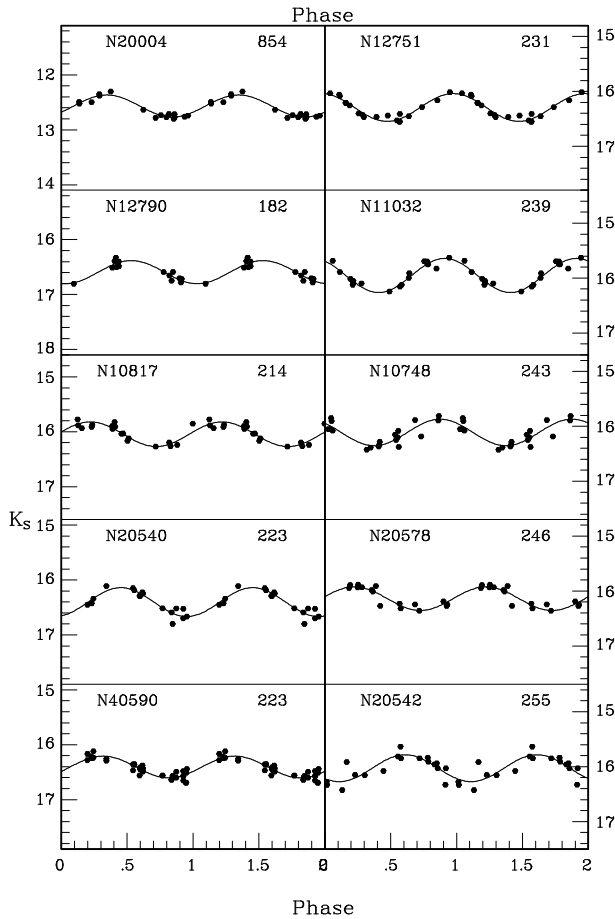
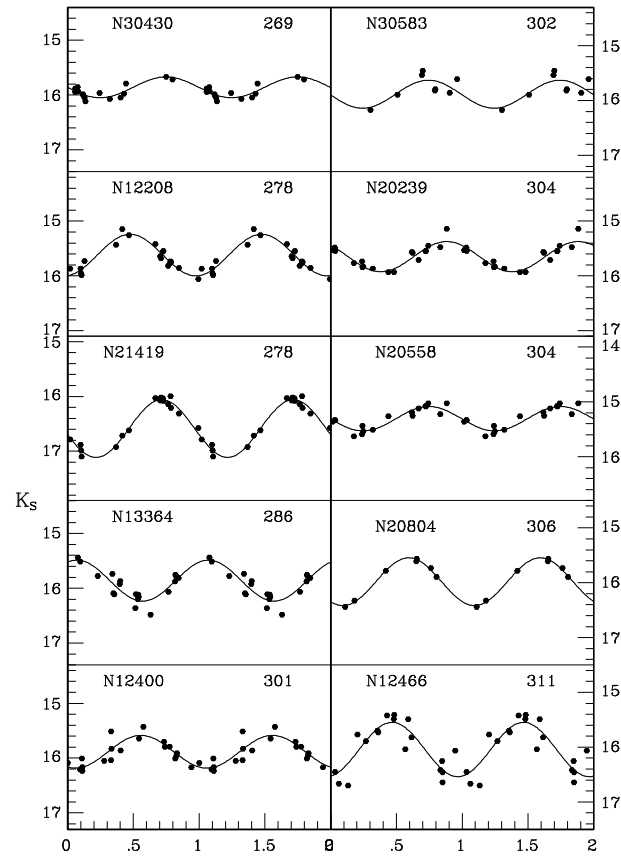
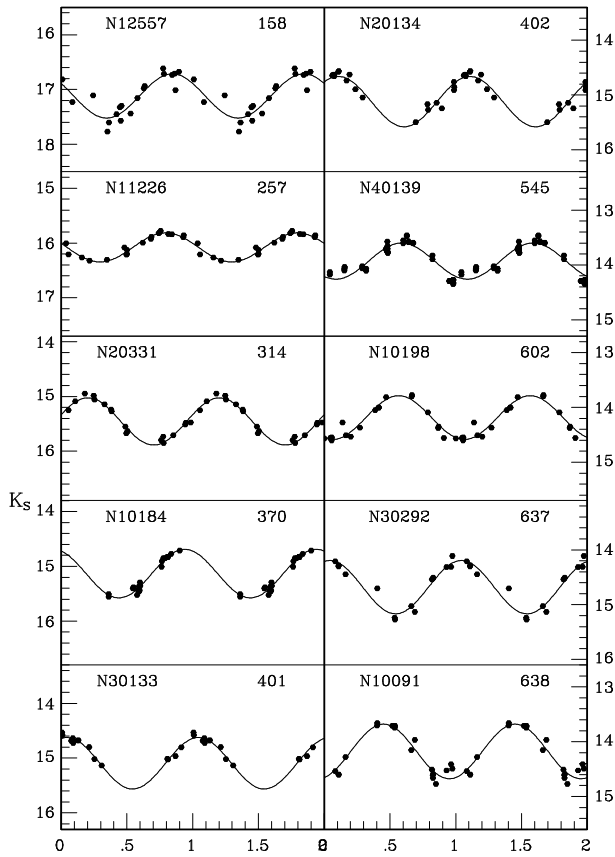


Figure 1. K_S light curves for the variables in Table 4(a)(b), arbitrarily phased (zero at JD2450000); each point is plotted twice to emphasize the variability. The best fitting first order curve

Figure 1. continued

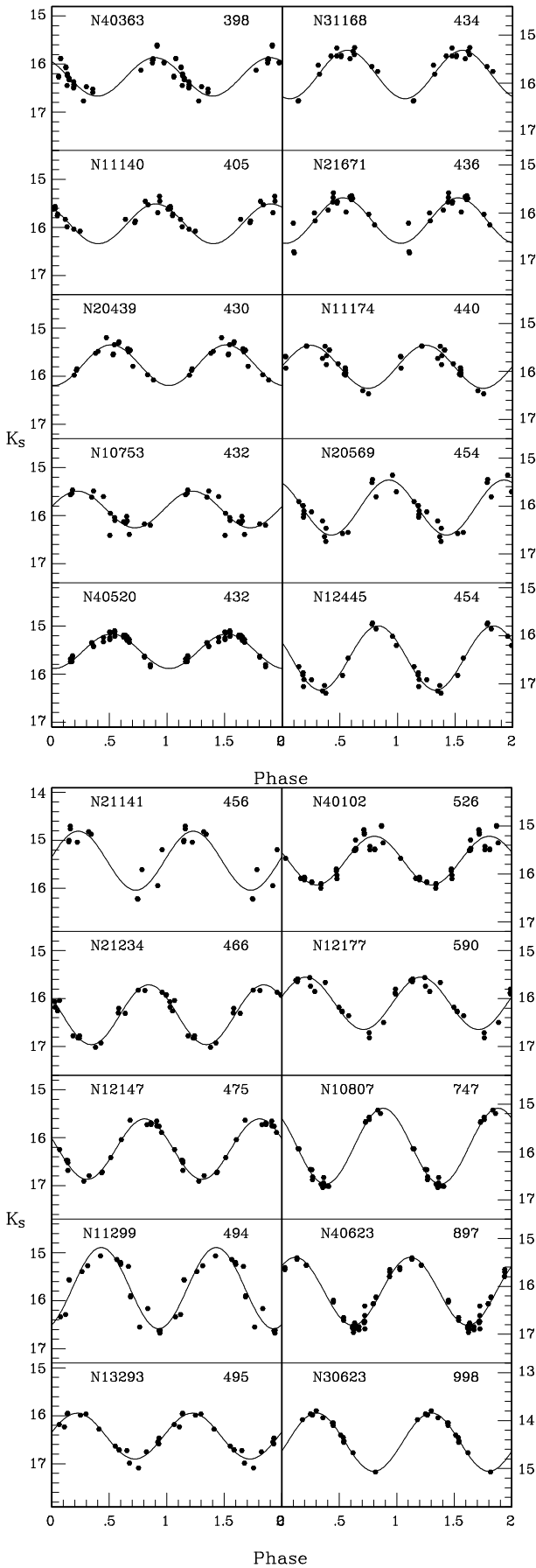


Figure 1. continued

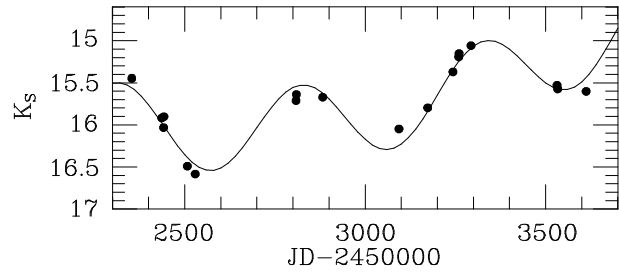


Figure 2. K_S light curve for N21029. The fitted curve is a combination of two sinusoids, one with $P=501$ days, representing the pulsation, the other with $P=5000$ days, representing a long-term trend. The latter is not a true period simply an indication that there are secular or long period changes in addition to the pulsation.